

## Existence of receding and advancing contact lines

Jens Eggers<sup>a)</sup>

*School of Mathematics, University of Bristol, University Walk, Bristol BS8 1TW, United Kingdom*

(Received 18 January 2005; accepted 30 June 2005; published online 18 August 2005)

We study a solid plate plunging into or being withdrawn from a liquid bath to highlight the fundamental difference between the local behavior of an advancing or a receding contact line, respectively. It is assumed that the liquid partially wets the solid, making a finite contact angle in equilibrium. In our hydrodynamic description, which neglects the presence of the outer gas atmosphere, an advancing dynamic wetting line persists to arbitrarily high speeds. The receding wetting line, on the other hand, vanishes at a critical speed set by the competition between viscous and surface tension forces. In the advancing case, we apply existing matching techniques to the plunging plate geometry to significantly improve on existing theories. For the receding contact line, we demonstrate for the first time how the local contact line solution can be matched to the far-field meniscus. In doing so, we confirm our very recent criterion for the vanishing of the receding contact line, leading to the formation of a film covering the solid. The results of both the advancing and the receding cases are tested against simulations of the full model equations. © 2005 American Institute of Physics. [DOI: 10.1063/1.2009007]

### I. INTRODUCTION

A number of recent experiments<sup>1-4</sup> have tested the stability of forced advancing and receding contact lines under conditions of partial wetting. For example, if a solid plate or fiber is plunging into a liquid bath to be coated (advancing contact line), the speed can be quite high (m/s) (Ref. 4) while maintaining a stationary contact line. In the opposite case of withdrawal (receding contact line),<sup>2</sup> a stationary contact line is observed only for very low speeds, and a macroscopic film is deposited,<sup>2,5</sup> typically at a speed of only a few cm/s.

The description of a moving contact line is complicated by the fact that the Navier-Stokes equation with standard no-slip boundary conditions<sup>6</sup> breaks down near it, because such a hypothetical flow would produce an infinite energy dissipation.<sup>7</sup> Instead, some microscopic length scale must be invoked that cuts off this singularity, which in this paper we are going to take as a slip length  $\lambda_{\text{slip}}$ . As a result, the local flow near the contact line is characterized by a typical length of about a nanometer,<sup>8</sup> which has to be matched<sup>9</sup> to the macroscopic flow away from the solid. In this paper, we apply a matching method developed for spreading drops<sup>10</sup> to the plunging plate, and test the result by comparing to numerical simulations. This very significantly improves the results of earlier calculations for the same problem.<sup>11,12</sup> For the opposite case of a receding contact angle we find that a new matching procedure is needed. The matching breaks down above a critical contact line speed, in agreement with our earlier results.<sup>13</sup>

Figure 1 illustrates the geometry to be considered in the present paper. On the left, a solid plate is pushed into a pool of viscous liquid. As a result, the interface deforms and the contact line is pushed downward relative to its equilibrium

position. Within the present model, this advancing contact line is stable at any speed. If the plate is withdrawn from the bath, fluid is pulled up with the plate, and a new contact line position is established. However, this state is realizable only at speeds below a critical speed  $U_c$ . For  $U > U_c$ , the contact line is no longer sustainable and continues to move up the plate.<sup>14</sup> In the stationary state, the plate is covered by a thin film, first described by Landau, Levich, and Derjaguin (LLD).<sup>15,16</sup> To understand the fundamental difference between pushing a plate and pulling it out, one has to consider the matching between the region very close to the contact line, and the capillary profile away from it. Qualitatively, the difference in the behavior of the advancing and of the receding contact line makes sense: If the plate is pushed into the liquid, the interface is bent away from the solid, and typical velocity gradients  $U/h_{\text{film}}$  are decreased. As a result, viscous forces, which tend to push the contact line farther into the liquid, are reduced. If the plate is pulled, on the other hand, the interface is pulled toward the solid, making the film thinner and enhancing viscous effects. Hence in the latter case there is a positive feedback, increasing the viscous pull, and thus leading to the disappearance of the contact line.

The strong energy dissipation near a moving contact line results from the fact that viscous forces become very large as the thickness of the liquid film goes to zero.<sup>7</sup> As a result of the interplay between viscous and surface tension forces, the interface is highly curved, and the contact line speed  $U$  is properly measured by the capillary number  $\text{Ca} = U\eta/\gamma$ , where  $\eta$  is the viscosity of the fluid and  $\gamma$  the surface tension between fluid and gas. Owing to this bending the interface angle measured at, say, 100  $\mu\text{m}$  away from the contact line differs<sup>17-20</sup> significantly from the microscopic angle directly at the contact line.

A convenient reference length for the present problem is the capillary length  $\ell_c = \sqrt{\gamma/(\rho g)}$ , which is about a millimeter for most liquids. Throughout this paper, all lengths will be

<sup>a)</sup>Electronic mail: jens.eggerts@bristol.ac.uk

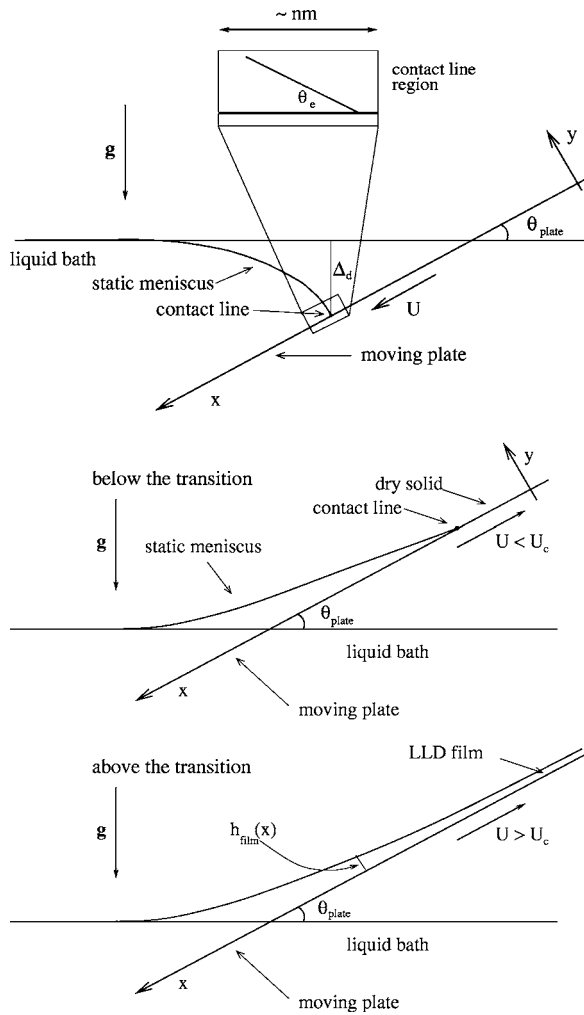


FIG. 1. A schematic of the setup: A plate is being withdrawn at an angle  $\theta_{\text{plate}}$  in the bottom two diagrams and being pushed into the fluid in the top diagram. Only the flow to the left-hand side of the plate is considered, which is assumed long enough for the coupling to the other side to be ignored. At the contact line, the microscopic slope of the interface is  $h'_{\text{film}}(0) = \theta_c$ . Since the interface is highly curved, this microscopic contact angle is only observed on a scale of nanometers (expanded region in the top diagram). The depression of the advancing contact line (top) relative to the level of the liquid bath is  $\Delta_d$ . The contact line is stable at any speed, while for the receding contact line (bottom) there exists a critical speed  $U_c$  above which the contact line vanishes. Instead, the plate is covered by a thin film.

nondimensionalized using  $\ell_c$ . The existence of a slip length  $\lambda_{\text{slip}}$ , which is of the order of a few molecular diameters under normal circumstances,<sup>21–23</sup> implies a convenient separation of length scales between the two parts of the surface profile. On one hand, there is a contact line region whose typical scale is  $\lambda_{\text{slip}} \approx 10^{-6}$ , on the other hand, there is an “outer” meniscus region, whose typical length scale is of order one.

All of the mathematical description to be presented in this paper uses the “lubrication approximation,” which relies on the assumption that the film slope, and in particular, the equilibrium contact angle  $\theta_e$  is small. This makes it convenient to normalize the film thickness by  $\theta_e$ , and to introduce the new variable  $h(x) = h_{\text{film}}(x)/\theta_e$  as well as  $\lambda = \lambda_{\text{slip}}/\theta_e$ .

Owing to the smallness of  $\lambda$ , which sets the scale near the contact line, one expects the local “inner” behavior of the

profile near the contact line to be of the form

$$h_{\text{in}}(x) = 3\lambda H\left(\frac{x}{3\lambda}\right), \quad \xi = \frac{x}{3\lambda}. \quad (1)$$

First one finds from (1) that the curvature of the interface is  $h''(x) = H''(\xi)/(3\lambda)$ , which becomes large for  $\lambda \rightarrow 0$  as expected, while the slope is  $h'(x) = H'(\xi)$ . The inner solution (1) has to be matched to an outer solution  $h_{\text{out}}(x)$ , whose curvature is of order 1, which means we have to join the two solutions at some scale  $\epsilon$  with  $1 \gg \epsilon \gg \lambda$ . This implies that the argument of  $h_{\text{out}}$  can effectively be taken at  $x=0$ , while  $\epsilon/(3\lambda) \gg 1$ . Thus in the limit  $\lambda \rightarrow 0$  (while keeping  $\epsilon$  fixed), the matching condition is

$$h''_{\text{out}}(0) = H''(\infty)/(3\lambda), \quad (2)$$

where the right-hand side corresponds to the leading-order term. Equation (2) ensures that the inner and the outer solutions are compatible. We will see that it needs to be supplemented by what is essentially a condition for the slope.

The matching condition (2) is the key to understanding dynamic wetting behavior. Let us summarize the main results of this paper by analyzing the solution qualitatively for the two cases of an advancing contact angle (plate plunging into the fluid) and of a receding contact angle (plate being withdrawn). For very small  $\lambda$ , it is clear that  $H''(\infty)$  must be small for matching to be possible, so in the limit,  $H''(\infty) = 0$  becomes the boundary condition for the inner problem. We will see that for an advancing contact angle, this boundary condition yields the inner scaling function  $H(\xi)$ , first found by Voinov.<sup>24</sup> The matching to Voinov’s solution is slightly complicated by the presence of logarithmic terms in the slope.<sup>10</sup>

On the other hand, Voinov’s solution cannot be applied to the case of a receding contact line. Rather, all inner solutions maintain a finite curvature  $H''(\infty) > 0$ . This means that at too small a value of  $\lambda$  the matching condition Eq. (2) can no longer be obeyed and the inner and the outer solutions are incompatible. As a result, the contact line vanishes. In a typical experiment,  $\lambda$  is constant and the speed is increased, but the effect is the same: Since the curvature of the interface is caused by viscous forces,<sup>7</sup>  $H''(\infty)$  increases with speed and matching becomes impossible. This explains the phenomenology described in Fig. 1. The impossibility of matching a receding contact line above a critical capillary number was already noticed in Ref. 25, based on numerical integration of the thin-film equations. Analytical solutions for the inner solution will permit us to give a much more complete description.

In Sec. II, we will introduce the hydrodynamic equations to be used for the calculation of stationary profiles. In Sec. III, we consider the case of a solid plate being pushed into the liquid (advancing contact angle). By matching an inner to an outer solution, we compute the profile as a function of speed. In Sec. IV, we introduce the matching procedure for the opposite case of a plate being withdrawn (receding contact angle). The failure of this matching procedure gives the critical capillary number at which the contact line can no longer exist, in agreement with our earlier result.<sup>13</sup> For speeds below the critical value, we again find the interface

profile. All our analytical results are tested by comparison with numerical solutions of the original equations. Finally, we summarize our results and indicate directions of future research.

## II. LUBRICATION DESCRIPTION

As illustrated in Fig. 1, we are considering a plate being pushed into or being withdrawn from a liquid bath at an angle  $\theta_{\text{plate}}$ . We have to solve the steady Navier–Stokes equation with a free surface, and no-slip boundary conditions on the plate. Since the plate is moving with speed  $U$ , the contact line between fluid, solid, and gas is moving relative to the solid. As explained above, the Navier–Stokes equation does not allow such a solution, and a small-scale cutoff has to be introduced at the contact line.<sup>17,18</sup> The dominant mechanism responsible for cutoff depends on the particular system under study.<sup>18,26</sup> As a representative example, we assume that the corner singularity is relieved by allowing the fluid to slip across the solid surface, since the matching to the slip region of size  $\lambda_{\text{slip}}$  is well understood in this case.<sup>10</sup> According to the Navier slip law,<sup>7</sup> the fluid speed relative to the solid is proportional to the shear rate:

$$u(x,0) - U = \lambda_{\text{slip}} \frac{\partial u}{\partial y} \quad \text{at } y=0. \quad (3)$$

Recently, we found<sup>27</sup> that various modifications of (3) have a minimal influence on the interface away from the contact line. Hence we do not believe that the particular cutoff mechanism used is of great importance.

A much thornier issue is the slope  $h'(0)$  of the fluid layer to be specified at the contact line. It is well appreciated that molecular processes are involved,<sup>28,29</sup> which are beyond a hydrodynamic description. This will lead to an effective speed dependence of the contact angle as defined on a scale of nanometers. The importance of these microscopic effects relative to hydrodynamic ones is determined by the amount of energy dissipation involved in either process.<sup>30</sup> Thus for high viscosities the speed dependence of the microscopic angle can most likely be ignored, in agreement with experimental data.<sup>31</sup> If there is no “intrinsic” speed dependence of the microscopic angle, then it must coincide with its equilibrium value  $\theta_e$  at zero speed. We thus take  $h'(0)=1$ , recalling the previous normalization of the film thickness.

Apart from our earlier assumption of  $\theta_e$  being small, we require that the plate angle  $\theta_{\text{plate}}$  be small as well, which we normalize according to  $\theta = \theta_{\text{plate}}/\theta_e$ . If viscosity is sufficiently large for inertia to be ignored, we can use the lubrication approximation<sup>10,14</sup> to find an equation in terms of the free-surface profile  $h(x)$  alone:

$$\frac{\pm \delta}{h^2 + 3\lambda h} = h''' - h' + \theta, \quad (4)$$

where we have introduced the reduced capillary number  $\delta = 3Ca/\theta_e^3$ . To distinguish more clearly between advancing and receding contact lines we always take  $\delta$  as a positive quantity and rather change the sign in the equation. The minus (–) sign corresponds to the plate plunging into the liquid,

the plus (+) sign to the opposite case of the plate being withdrawn.

Viscous forces appear on the left-hand side of (4) (proportional to the speed), and diverge quadratically as  $h$  goes to zero at the contact line. As a result, viscous dissipation would diverge if it were not for the presence of slip, which weakens the singularity. Near the contact line the surface is highly curved, so the first term on the right-hand side of Eq. (4), which comes from surface tension, balances the viscous term on the left-hand side. The other two terms stem from gravity and only come into play at greater distances from the contact line. The film thickness vanishes at the contact line, where the slope is  $h'(0)=1$  as discussed above. Far away from the plate, the surface coincides with the liquid bath, so the third boundary condition is  $h'(\infty)=\theta$ .

## III. PUSHING

We begin by considering a plate being pushed into a viscous fluid, corresponding to the – sign in (4). In the spirit of the matching condition (2), we approach this problem by first considering the leading-order behavior near the contact line, where  $h$  goes to zero. As discussed above, this equation<sup>10</sup> is

$$\frac{-\delta}{h^2 + 3\lambda h} = h''', \quad (5)$$

which we studied in detail in Ref. 27 for a more general class of slip models. The characteristic scale of the local solution is the slip length  $\lambda$ , so it is convenient to introduce the scaled variables Eq. (1), which leads to

$$\frac{\delta}{H^2 + H} = -H'''. \quad (6)$$

As argued above, the matching condition (2) leads to the requirement that the curvature  $H''(\xi)$  vanishes for large  $\xi$  as the limit  $\lambda \rightarrow 0$  is performed. This means that the boundary conditions for the solution of (6) are

$$H(0) = 0, \quad H'(0) = 1, \quad H''(\infty) = 0. \quad (7)$$

The only parameter now appearing in the problem is the rescaled capillary number  $\delta$ , and Eqs. (6) and (7) uniquely specify the profile close to the contact line.

This inner solution can be found by expanding in a power series in the capillary number in a manner described in many papers.<sup>10,27,32</sup> If one writes the solution in terms of  $h'^3$ , its behavior for large  $x/\lambda$  is

$$h_{\text{in}}'^3(x) - 1 = 3\delta \ln(x/L) \quad (8)$$

to any order in the capillary number.<sup>27</sup> This is the form originally proposed by Voinov,<sup>24</sup> using more qualitative arguments. The length  $L$  appearing inside the logarithm can be computed as a power series in the capillary number:

$$L = \frac{3\lambda}{e} \left( 1 - \frac{\pi^2 - 1}{6} \delta + O(\delta^2) \right), \quad (9)$$

but for simplicity we only take the leading-order term into account in this paper, as corrections introduced by the next order are usually quite small.<sup>27</sup>

The crucial point of representing the inner solution in the form (8) is that the only parameter multiplying  $\ln(x)$  is the capillary number, which is defined in terms of the “outer” problem. Namely, the outer problem (8) needs to be matched to is

$$\frac{-\delta}{h_{\text{out}}^2} = h_{\text{out}}''' - h_{\text{out}}' + \theta, \tag{10}$$

which does not contain a contact line parameter like  $\lambda$ . Owing to the strong singularity for  $h \rightarrow 0$ ,<sup>7,10</sup> (10) does not have a solution with finite slope at the contact line  $h_{\text{out}}(0)=0$ , making it impossible to impose a slope. Instead, we are seeking a solution to (10) that has the form (8) for  $x \rightarrow 0$ ; in other words,

$$h_{\text{out}}'''(x) = 3\delta \ln(x) + F, \quad x \rightarrow 0, \tag{11}$$

where  $F$  is a constant to be computed. As demonstrated in Ref. 10, this can be achieved by expanding the outer solution in a power series in  $\delta$ :

$$h_{\text{out}}(x) = h_0(x) + \delta h_1(x) + O(\delta^2). \tag{12}$$

The equation for  $h_0$ , representing a balance of surface tension and gravity, is

$$h_0''' - h_0' + \theta = 0. \tag{13}$$

Equation (13) has the following family of solutions, which are growing linearly at infinity and which vanish at the contact line:

$$h_0(x) = \theta x + (\theta - \theta_{\text{ap}})(e^{-x} - 1). \tag{14}$$

The slope  $h_0'(0) = \theta_{\text{ap}}$  of (14) at the contact line is called the “apparent” contact angle (normalized by  $\theta_e$ ) and is a free parameter still to be determined by the matching procedure. Its name is motivated by the fact that a macroscopic measurement of the profile on a scale of order one will yield a profile close to (14). If extrapolated to the contact line, the angle will appear to be  $\theta_{\text{ap}}$ , rather than the true microscopic value 1. Obviously, (14) cannot be matched directly to the contact line solution (8), which contains a logarithm. This logarithmic dependence will come out of the next-order solution  $h_1$ , whose equation reads

$$h_1''' - h_1' = f(x), \quad f(x) = -1/h_0(x)^2. \tag{15}$$

The solution is straightforward:<sup>33</sup>

$$h_1(x) = -\frac{e^x}{2} \int_1^\infty e^{-t} f(t) dt + \int_1^x [\cosh(t-x) - 1] f(t) dt + Ke^{-x} + K_2, \tag{16}$$

where once more any particular solution that is growing at infinity was suppressed, and  $K, K_2$  are constants of integration. To find  $K, K_2$ , we note that  $h$  must vanish at the contact line, giving the first condition  $h_1(0)=0$ . To compute  $h_1(0)$ , we observe that the second integrand of (16) can be expanded like  $\cosh(t-x) - 1 = \cosh(t) - 1 - x \sinh(t) + O(x^2)$ . The term linear in  $x$  does not contribute for small  $x$ , since  $\sinh(t)f(t)$  behaves like  $1/t$  for small arguments, and hence

$$\lim_{x \rightarrow 0} x \int_1^x \sinh(t) f(t) dt = 0.$$

Thus one finds

$$0 = h_1(0) = -\frac{1}{2} \int_1^\infty e^{-t} f(t) dt + \int_0^1 [1 - \cosh(t)] f(t) dt + K + K_2, \tag{17}$$

where the singularity of  $f(t) \propto 1/t^2$  cancels out to make the second integral convergent.

Next we find a condition at infinity by noting that

$$h(x) = \theta x + \Delta + O(1/x), \tag{18}$$

where  $\Delta$  is the vertical distance of the contact line from the undisturbed surface, normalized by  $\theta_e$ . Since we want  $h_0$  to represent the far-field behavior of the profile, we put  $h_1(\infty) = 0$ , and thus  $\Delta = \theta_{\text{ap}} - \theta$ , by comparison with (14). This means we have

$$0 = h_1(\infty) = \lim_{A \rightarrow \infty} \left( \frac{e^{-A}}{2} \int_1^A e^t f(t) dt \right) - \int_1^\infty f(t) dt + K_2.$$

The first of the three terms on the right-hand side is zero, as one confirms by splitting it into two parts:

$$\lim_{A \rightarrow \infty} \left( \frac{e^{-A}}{2} \int_1^B e^t f(t) dt + \frac{e^{-A}}{2} \int_B^A e^t f(t) dt \right),$$

where  $B$  is a large positive constant. The first of the two parts is evidently zero, for the second one notes that the argument can be approximated as  $e^t f(t) \approx -e^t / (\theta^2 t^2)$  for large  $t > B$ , whose absolute value has the upper bound  $e^A / (\theta^2 A^2)$ . Thus in the limit the second part vanishes as well. Using (17) this means the constant  $K$  in (16) can be computed as

$$K = \int_1^\infty \left( \frac{e^{-t}}{2} - 1 \right) f(t) dt + \int_0^1 [\cosh(t) - 1] f(t) dt. \tag{19}$$

We are now in a position to determine the constant  $F$  in Eq. (11). Comparing (11) to (12), we know that for small  $x$  the first-order contribution  $h_1'$  must have a logarithmic singularity of the form

$$h_1'(x) \approx 1/\theta_{\text{ap}}^2 \ln(x) + C(\theta/\theta_{\text{ap}})/\theta_{\text{ap}}^2. \tag{20}$$

Namely, for small  $x$ ,

$$3\delta \ln(x) + F \approx h_{\text{out}}'''(x) \approx [h_0'(x) + \delta h_1'(x)]^3 \approx \theta_{\text{ap}}^3 + 3\delta \ln(x) + 3\delta C(\theta/\theta_{\text{ap}}) + O(\delta^2),$$

so that  $F = \theta_{\text{ap}}^3 + 3\delta C(\theta/\theta_{\text{ap}}) + O(\delta^2)$ . Analysis of (16) for  $x \rightarrow 0$  gives, using (19) and  $f(t) \approx -1/(\theta_{\text{ap}} t)^2$  for small  $t$ ,

$$C(\theta/\theta_{\text{ap}}) = \int_1^\infty (1 - e^{-t}) f(t) \theta_{\text{ap}}^2 dt + \int_0^1 [(1 - e^{-t}) f(t) \theta_{\text{ap}}^2 + 1/t] dt + 1. \tag{21}$$

This completely determines the outer solution (12). Comparing it to the inner solution (8), we finally obtain



$$\theta_{ap}^3 + 3\delta C(\theta/\theta_{ap}) = 1 - 3\delta \ln(L), \tag{22}$$

which is an equation to be solved for the apparent contact angle  $\theta_{ap}$ . The equation for  $\theta_{ap}$  can be simplified considerably by observing that  $\theta_{ap} = 1 + O(\delta)$ , so it is consistent to replace  $C(\theta/\theta_{ap})$  by  $C(\theta)$  in Eq. (22). Thus we obtain the explicit expression

$$\theta_{ap}^3 = 1 - 3\delta \ln(cL), \tag{23}$$

with  $c = \exp[C(\theta)]$ , in agreement with the general analysis of.<sup>34</sup> A major advantage of (22), though, is that it can be applied in a situation of complete wetting  $\theta_e = 0$ . A more detailed analysis of this case is however outside the scope of this paper.

To test the result of our matching procedure (22) and of the simplified version (23), we compare the depression  $\Delta = \theta_{ap} - \theta$  of the meniscus with the result of a numerical solution of the original (4). Remarkably, the prediction, which contains no adjustable parameters, remains extremely good up to a reduced capillary number of  $\delta = 1$ . The full (22), which keeps some higher-order terms in  $\delta$ , performs slightly better than (23). To further appreciate the quality of the agreement, we plotted the result of an earlier theory<sup>11</sup> as the dotted line. In this earlier theory, a perturbation expansion of (4) in  $\delta$  is matched directly to a linearized version of (8). However, the expansion is performed around the static profile corresponding to zero speed, whereas our expansion is around  $h_0(x)$ , which already incorporates a speed-dependent deformation of the surface.

Effectively, this amounts to approximating the result of (23) according to

$$\Delta = \theta_{ap} - \theta = [1 - 3\delta \ln(cL)]^{1/3} - \theta \approx 1 - \theta - \delta \ln(cL). \tag{24}$$

For the special case  $\theta = 1$ , one finds  $C(1) = \gamma$ , where  $\gamma$  is Euler's constant. This gives the result of<sup>11</sup>

$$\Delta = -\delta [\ln(L) + \gamma], \tag{25}$$

shown as the dotted line in Fig. 2. The profile  $h'(x)$  obtained numerically agrees equally well with the outer solution (12), as shown in Fig. 3. It is only for  $x/\lambda \lesssim 1$  that the outer solution begins to fail, since it has a logarithmic singularity at the origin.

**IV. PULLING**

We now turn to the opposite case of a plate being withdrawn from a bath, for which the left-hand side of (4) is now positive. The dominant balance close to the contact line is again between the term on the left-hand side of (4) and the first term on the right-hand side. With the similarity transformation (1), this is converted into

$$\frac{\delta}{H^2 + H} = H''', \tag{26}$$

which differs from (6) only by a sign. However, the behavior of the solution of (26) as  $\xi \rightarrow \infty$  is completely different. This is best appreciated by considering the limiting form of (26) for  $H \gg 1$  (away from the contact line):

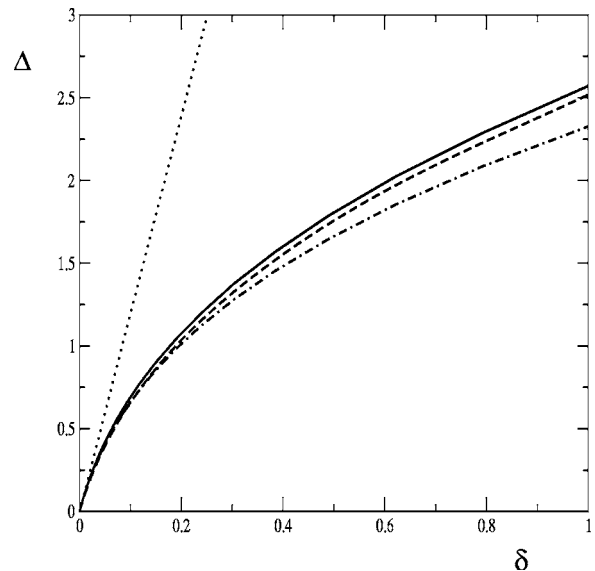


FIG. 2. The normalized depression  $\Delta$  of the meniscus, as function of the reduced capillary number  $\delta$ . The slip parameter is  $3\lambda = 10^{-5}$ , and  $\theta = 1$ . The full line is the result of a numerical solution of (4), the dashed line is our theoretical result (22), using  $\Delta = \theta_{ap} - \theta$ . The dot-dashed line is the simplified equation (23). The dotted line is the theoretical result of Ref. 11.

$$\frac{1}{y^2} = y''', \tag{27}$$

where we have put  $H(\xi) = \delta^{1/3} y(\xi)$ .

Remarkably, this equation has an exact solution, whose properties have been summarized in Ref. 35. In parametric form, a solution with  $y(0) = 0$  reads

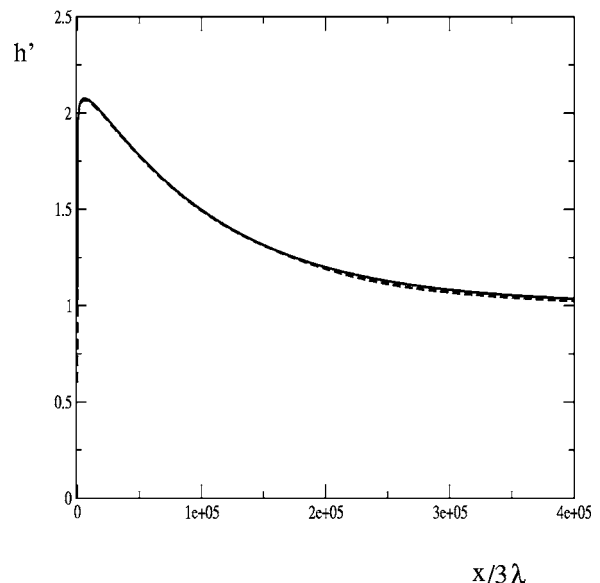


FIG. 3. A comparison between a profile obtained numerically by integrating (4) for  $\delta = 0.3$  and the outer solution (12). The other parameters are those of Fig. 2. For  $\delta = 0.3$ , (22) gives  $\theta_{ap} = 2.32$ .

$$\left. \begin{aligned} \xi &= \frac{2^{1/3} \pi \text{Ai}(s)}{\beta[\alpha \text{Ai}(s) + \beta \text{Bi}(s)]} \\ y &= \frac{1}{[\alpha \text{Ai}(s) + \beta \text{Bi}(s)]^2} \end{aligned} \right\} s \in [s_1, \infty[, \quad (28)$$

where Ai and Bi are Airy functions.<sup>36</sup> The limit  $\xi \rightarrow 0$  corresponds to  $s \rightarrow \infty$ , the opposite limit  $\xi \rightarrow \infty$  to  $s \rightarrow s_1$ , where  $s_1$  is a root of the denominator of (28):

$$\alpha \text{Ai}(s_1) + \beta \text{Bi}(s_1) = 0. \quad (29)$$

Since the solution extends to  $s = \infty$ ,  $s_1$  has to be the largest root of (29).

From (28), the behavior of  $y(\xi)$  for large  $\xi$  can be obtained<sup>35</sup> [note that there is a misprint in Eq. (12) of Ref. 35]:

$$y'(\xi) = \kappa_y \xi + b_y + O(\xi^{-1}), \quad (30)$$

where

$$\kappa_y = \left( \frac{2^{1/6} \beta}{\pi \text{Ai}(s_1)} \right)^2, \quad b_y = \frac{-2^{2/3} \text{Ai}'(s_1)}{\text{Ai}(s_1)}.$$

The constant  $\beta$  can be determined by matching (28), which is valid only for  $\xi \geq 1$ , to a solution of (26), which includes the effect of the cutoff and is thus valid down to the position  $\xi = 0$  of the contact line. The limit of (28) for small values of  $\xi$  gives<sup>35</sup>

$$H'^3(x) = \delta y'^3(\xi) \approx 3 \delta \ln[\pi / (2^{2/3} \beta^2 \xi)], \quad (31)$$

which remains valid for  $\xi \leq \beta^{-2}$ . Thus, (31) is a valid solution of the full equation (26) for  $1 \leq \xi \leq \beta^{-2}$ .

Following Refs. 10 and 27, we compare (31) to the expansion of the full equation (26) in  $\delta$ . Using the boundary conditions  $H(0) = 0$  and  $H'(0) = 1$ , one finds

$$H'(\xi) = 1 + \delta \{ \xi [\ln(\xi) - \ln(\xi + 1)] - \ln(\xi + 1) + C \xi \} + O(\delta^2). \quad (32)$$

Since this solution has to match the logarithmic behavior (31), we put the constant of integration  $C$  to zero, and (32) becomes, for  $\xi \geq 1$ ,

$$H'^3(\xi) = 1 - 3 \delta \ln(\xi) + O(\delta^2). \quad (33)$$

Thus, comparing (33) to (31), we find

$$\beta^2 = \pi \exp[-1/(3\delta)] / 2^{2/3} + O(\delta). \quad (34)$$

For  $\delta \ll 1$ ,  $\beta$  is indeed exponentially small, and (28) has a logarithmic dependence over a large range of  $\xi$  values:  $1 \leq \xi \leq \exp[1/(3\delta)]$ . This makes it possible to match (28) to (33) in the limit  $\xi \gg 1$ , although the ultimate behavior of (28) for large  $\xi$  is given by Eq. (30).

We are now in the position to match the inner solution of (26), which has the form (1) to an appropriate outer solution, following the prescription (2) given in the Introduction. To achieve this matching it is enough to consider  $h_{\text{out}}(x) = h_0(x)$  as given by (14), since (30) does not contain any logarithmic term. For  $x/\lambda \gg 1$ , the solution of (26) is well described by (28), so we have

$$h_{\text{out}}(x) = \theta x + (\theta - \theta_{\text{ap}})(e^{-x} - 1), \quad (35a)$$

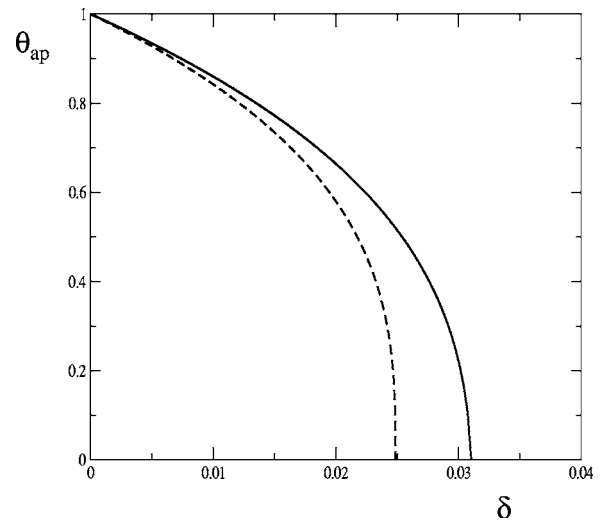


FIG. 4. The full line is the apparent contact angle  $\theta_{\text{ap}}$  according to (39). The other parameters are  $\lambda = 10^{-6}$  and  $\theta = 2$ . The dashed curve is the approximation (46), valid for small capillary number. The apparent contact angle goes to zero at the critical reduced capillary number  $\delta_{\text{cr}} = 0.031$ . At the transition the slope of the full line is given by (48), the dashed line has a vertical tangent.

$$h_{\text{in}}(x) = 3\lambda \delta^{1/3} y[x/(3\lambda)], \quad (35b)$$

where  $y(\xi)$  is given by (28) and (34). The matching procedure must supply us with the parameter  $s_1$  in (28), which is yet to be determined.

The matching works in the limit  $\lambda \rightarrow 0$ , for which we require that the expansions

$$h'_{\text{out}}(x) = \theta_{\text{ap}} + (\theta - \theta_{\text{ap}})x + O(x^2), \quad (36)$$

$$h'_{\text{in}}(x) = \delta^{1/3} [\kappa_y x / (3\lambda) + b_y] + O(\lambda/x)$$

agree, or

$$\theta_{\text{ap}} = \delta^{1/3} b_y, \quad (37a)$$

$$\theta - \theta_{\text{ap}} = \delta^{1/3} \kappa_y / (3\lambda). \quad (37b)$$

Eliminating  $\theta_{\text{ap}}$  between Eqs. (37a) and (37b) we finally have

$$\frac{\theta}{\delta^{1/3}} + \frac{2^{2/3} \text{Ai}'(s_1)}{\text{Ai}(s_1)} = \frac{\exp[-1/(3\delta)]}{3 \cdot 2^{1/3} \pi \text{Ai}^2(s_1) \lambda}, \quad (38)$$

which should be read as an equation for  $s_1$ . Once  $s_1$  is known, all remaining parameters in  $h_{\text{in}}$  and  $h_{\text{out}}$  can be found. For example, from (37a) one finds the apparent contact angle to be

$$\theta_{\text{ap}} = \frac{-2^{2/3} \delta^{1/3} \text{Ai}'(s_1)}{\text{Ai}(s_1)}, \quad (39)$$

an example of which is plotted in Fig. 4. At some finite critical reduced capillary number  $\delta_{\text{cr}}$ ,  $\theta_{\text{ap}}$  goes to zero. Physical solutions cannot exist for capillary numbers beyond that, since the outer solution only makes physical sense for  $\theta_{\text{ap}} \geq 0$ . Following Ref. 13, we now derive a much simpler equation for the critical capillary number  $\delta_{\text{cr}}$  at which the contact line disappears, and show that it is equivalent to  $\theta_{\text{ap}} = 0$ .

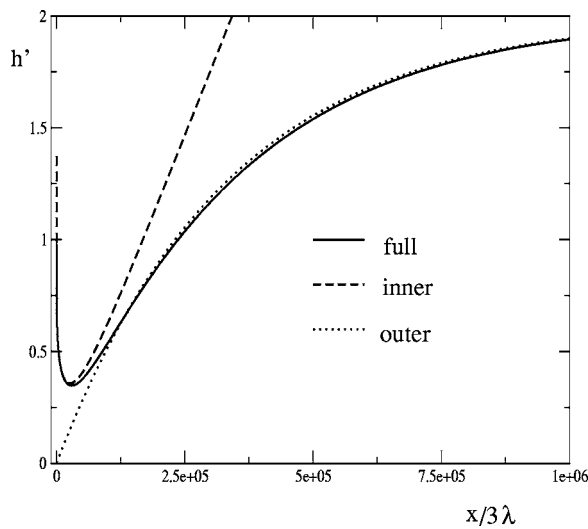


FIG. 5. A comparison of the full solution at the critical capillary number with the inner and outer solutions. We plot the slope of the interface, so  $h'(0)=1$  for the full solution, and  $h'(0)=0$  for the outer solution, consistent with the condition by Derjaguin and Levi. The other parameters are  $\lambda = 10^{-6}$  and  $\theta=2$ , so from (41) we obtain  $\delta=0.031$ .

Since  $\theta_{ap} \geq 0$ , the maximum value of the left-hand side of (37b), which is the curvature of the outer solution, is  $\theta$ . The right-hand side, corresponding to the curvature of the inner solution, is on the other hand bounded from below. From (30), it is seen that the minimum curvature corresponds to the condition that  $Ai(s_1)$  must be maximal among solutions of (29). By choosing  $\alpha = \alpha_{cr} \equiv -\beta Bi(s_{max})/Ai(s_{max})$ , we can in fact ensure that  $Ai$  assumes its global maximum 0.53566..., which occurs for  $s = s_{max} = -1.0188...$ . Thus we have singled out a unique solution of (27), which minimizes the curvature

$$\kappa_y^{cr} = \frac{\exp[-1/(3\delta)]}{2^{1/3} \pi [Ai(s_{max})]^2}, \quad (40)$$

the value of which increases with capillary number as expected.

Now by equating the maximum value of the left-hand side of (37b) with the minimum value of the right-hand side of (37b), we obtain an equation for a capillary number above which no solution can exist:  $\theta = \delta^{1/3} \kappa_y^{cr}/(3\lambda)$ , or explicitly

$$\delta_{cr} = \frac{1}{3} \left[ \ln \left( \frac{\delta_{cr}^{1/3}}{54^{1/3} \pi [Ai(s_{max})]^2 \lambda \theta} \right) \right]^{-1}. \quad (41)$$

But at the capillary number given by (41), the first matching condition (37a) is also satisfied identically. This is because  $Ai$  is extremal, so  $Ai' = 0$  and  $\theta_{ap} = b_y = 0$ . Thus  $\delta_{cr}$  as given by (41) gives exactly the critical capillary number corresponding to  $\theta_{ap} = 0$  in Fig. 4. This confirms a classical conjecture by Derjaguin and Levi,<sup>37</sup> later reiterated by others,<sup>38</sup> that the transition to a film is characterized by the apparent contact angle going to zero. This criterion was confirmed experimentally in Ref. 2 using fibers being pulled out of a viscous liquid.

In Fig. 5 we show the result of a numerical integration of (4) at the critical capillary number, and compare it to the

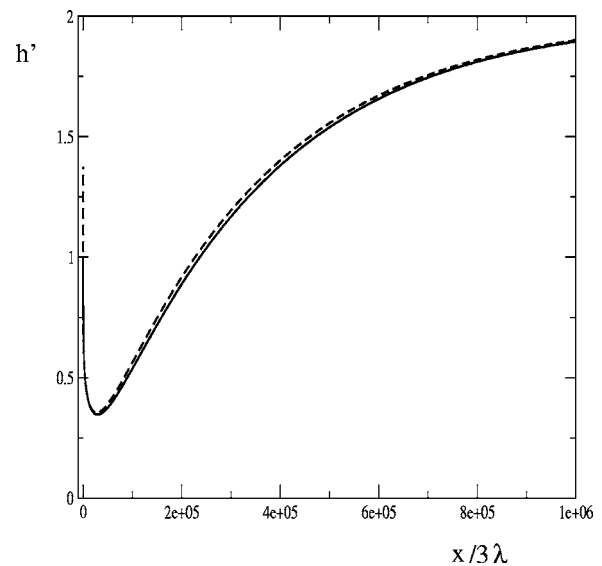


FIG. 6. The interface slope at the critical capillary number for  $\theta=2$  and  $\lambda = 10^{-6}$ . The full line is the result of the numerical integration at  $\delta_{cr} = 0.0309$ , while the theoretical prediction (41) gives  $\delta=0.0329$ . The dashed line is the composite solution (42).

inner and outer solutions (35). The critical capillary number was found numerically by raising  $\delta$  until no other solutions of (4) could be found. For large  $\xi$ , the slope of the outer solution (35a) agrees with the numerical solution, but extrapolates to  $h'=0$  at the contact line, as required by  $\theta_{ap} = 0$ . Coming from the interior, the inner solution (35b) agrees with the full solution up to the turning point.

To obtain a profile that is more uniformly valid, one can use a composite approximation.<sup>9</sup> The idea is to add the inner and outer solutions that have been matched, and to subtract the behavior (36) in the region in which the two solutions overlap:

$$h_{comp}(x) = h_{in}(x) + h_{out}(x) - [\theta_{ap} + (\theta - \theta_{ap})x]. \quad (42)$$

It is evident that  $h_{comp}$  agrees with the full solution for large  $x$  as well as for small  $x$ ; hence it will be the best global approximation at this order of the matching. This excludes the region  $\xi \lesssim 1$  where (35b) has a logarithmic singularity. Figure 6 illustrates the remarkable agreement of the composite solution with the full numerical result at the critical capillary number, where the approximation is expected to be worst.

Having studied the critical capillary number, let us return once more to the matching condition (38) which determines the solutions for  $\delta < \delta_{cr}$ . Namely, it is instructive to obtain explicit solutions of (38) in the limit of small  $\delta$ , in which case its solution  $s_1$  is large, and the asymptotics of the Airy function<sup>36</sup> gives

$$Ai(s) \approx e^{-2s^{3/2}/3} s^{-1/4}/(2\pi^{1/2}). \quad (43)$$

Thus, (38) becomes, for small  $\delta$ ,

$$\frac{\theta}{\delta^{1/3}} - 2^{2/3} s^{1/2} - \frac{2^{5/3} s^{1/2}}{3\lambda} e^{-1/(3\delta)+4s^{3/2}/3} \approx 0, \quad (44)$$

and (39) is

$$\theta_{\text{ap}} \approx \delta^{1/3} 2^{2/3} s^{1/2}. \quad (45)$$

In the simplest approximation the exponent in (44) must vanish,  $s = [1/(4\delta)]^{2/3}$ , and inserting this into (45) gives  $\theta_{\text{ap}} \approx 1$ . Not surprisingly, at very small capillary numbers the interface is hardly deformed at all.

To go beyond this approximation, we put  $s^{1/2} = [1/(4\delta) + \Delta s]^{1/3}$ , insert into (44), and analyze the result for small  $\delta$ , which gives

$$\Delta s \approx \frac{3}{4} \ln \left( \frac{3\lambda}{2} (\theta - 1) \right).$$

Putting this into (45) leads to the next approximation:

$$\theta_{\text{ap}}^3 \approx 1 - 3\delta \ln \left( \frac{2(\theta - 1)}{3\lambda} \right), \quad (46)$$

which has exactly the same form as (23) for the apparent contact angle in the advancing case. However, even for a small capillary number, the receding and the advancing case needs to be treated differently, as the constant inside the logarithm is different. For  $\theta = 1$ , the argument of the logarithm in (46) becomes singular, which means one has to go to an even higher order in the approximation, but we are not pursuing this special case here. The approximation (46) is plotted as the dashed line in Fig. 4. If extrapolated naively to  $\theta_{\text{ap}} = 0$ , it gives a surprisingly good estimate of  $\delta_{\text{cr}}$ .

However, there exists a more fundamental difference between (39) and (46), which is of relevance for perturbations of the contact line position around its stationary value.<sup>39</sup> Namely,

$$\tau^{-1} \approx -\theta_{\text{ap}}^{-1} \left. \frac{d\theta_{\text{ap}}}{d\delta} \right|_{\delta_{\text{cr}}} |k| \quad (47)$$

is an estimate of the relaxation time of a transversal perturbation of the contact line position at a wave number  $k$ . In the approximation (46) (dashed line in Fig. 4), the apparent contact angle goes to zero with a vertical tangent, resulting in a diverging relaxation time  $\tau$  as the transition toward a LLD film is approached. The same is true for de Gennes' description<sup>40</sup> of the transition (to be discussed in more detail below), which is used in Ref. 39.

In the present theory, however, the slope of  $\theta_{\text{ap}}(\delta)$  remains finite at the transition. It is a routine matter to expand Eqs. (38) and (39) for small deviations from the critical capillary number:  $\delta = \delta_{\text{cr}} + \delta_1$ . Without giving the details, which are straightforward, one obtains

$$\left. \frac{d\theta_{\text{ap}}}{d\delta} \right|_{\delta_{\text{cr}}} = -\theta [1/(2^{1/3} 3\delta_{\text{cr}}) + 1/(18^{1/3} \delta_{\text{cr}}^2)] < 0. \quad (48)$$

However, using the parameter values of Fig. 4, the slope is  $-811$ , so relaxation times are still quite large near the transition, probably sufficiently large for the theory<sup>39</sup> to work in practice.

## V. DISCUSSION

Let us begin by considering extensions and generalizations of the present theory in which the contact line remains straight. First, our arguments are not limited to a specific contact line model, since they are based entirely on hydrodynamic arguments away from the contact line. Namely, the thin-film equation (4) with  $\lambda = 0$  is valid at a distance from the contact line greater than the slip length or the range of van der Waals forces. Near the contact line, the profile is given by the leading-order solution (28). Its parameters have to be determined by matching to the contact line, as was done here in the case of the slip model. Another possible matching was described in Ref. 11 for the case that van der Waals forces are dominant near the contact line, which changes the parameter  $L$  appearing in (8) (advancing contact angle) or  $\beta$  in (31) (receding contact line). In the latter case, the slip length  $\lambda$  in (41) for the critical capillary number has to be replaced by  $\sqrt{A/(6\pi\gamma)/(6\theta_e^2)}$ , where  $A$  is the Hamaker constant. In more recent and detailed models of the contact line, the contact line singularity is relieved by recognizing that the interface is of finite thickness, and treating it according to van der Waals' theory.<sup>41</sup> However, the task of calculating the parameters of (28) in terms of microscopic parameters of the contact line still remains to be done for these more elaborate descriptions of the contact line. Another possible generalization of the present description is to cases where the equilibrium contact angle is not small, so that lubrication theory fails close to the contact line. In that case, the flow directly at the contact line would have to be described without resorting to lubrication theory,<sup>24,34</sup> but the relevant region where matching occurs is characterized by slopes  $h'(x)$ , which are small. Thus we anticipate that many essential features of the present calculation will carry over to the case of  $\theta_e$  not being small.

Second, one can generalize to a different geometry. To this end, one has to replace (14) by the appropriate static solution for the problem at hand. This is done almost trivially for the case of a vertical plate or a fiber,<sup>6</sup> in which case the lubrication description (4) is no longer valid far from the contact line, since  $\theta$  is not small. However, this does not pose a problem since this part of the profile is determined by surface tension and gravity alone. In the same spirit, the present model can be extended to a flow inside a capillary tube, with only very minor changes to the value of the critical capillary number.<sup>14</sup>

Third, one can consider dynamical effects, of particular interest for the unstable case of a receding contact line. In Ref. 14, it was found that when the stationary profile vanishes, it is not followed directly by the LLD film, which is of macroscopic thickness. Rather, there is a narrow range of speeds where the contact line is pulled up the plate, but at a speed that is smaller than  $U$ , i.e., the contact line is partially slipping. The thickness of the film that is left behind is in the order of  $\lambda$ , i.e., microscopic. Only when the speed is raised still further does the LLD film appear. So far these results are only numerical; a full analytical theory would be desirable. Note also that these transitions are strongly hysteretical. Once the LLD film has appeared, it can be sustained to much



lower capillary numbers than  $\delta_{cr}$ . It is usually assumed that the LLD film vanishes when its thickness has reached the range of intermolecular forces,<sup>5</sup> but we are not aware of any theoretical investigation of this problem.

Next we come to the experimental evidence. The most extensive experiments on the critical capillary number for a receding contact line were done with a capillary tube,<sup>1</sup> by pushing out a viscous liquid. Using a variety of different materials it was found that a film was deposited above a given value of the reduced capillary number  $\delta=3Ca/\theta_e^3$ , in agreement with the present theory. The actual value of the critical capillary number, however, is about a factor of 2 too low, if the theoretical estimates are based on  $\lambda_{slip}\sim 10^{-6}$ . Several possible explanations suggest themselves. First, the materials used in Ref. 1 have considerable contact angle hysteresis, pointing to surface roughness. This will tend to reduce the critical capillary number.<sup>39</sup> In addition, any speed dependence of the microscopic contact angle, neglected in the present description, will effectively lower  $\theta_e$  and thus lead to a smaller critical capillary number.

Our theory for the vanishing of the receding contact line has some similarities with an earlier theory,<sup>40</sup> in that the transition is predicted at a given value of the reduced capillary number [cf. (41)]. However, it differs in predicting a vanishing apparent contact angle at the transition, while it is  $\theta_{ap}=1/\sqrt{3}$  in Ref. 40. The approach of Ref. 40 is also different in that it considers the local problem in isolation, hence the dependence of  $\delta_{cr}$  on parameters of the outer problem like  $\theta$  cannot be captured. In fact, we believe that the mechanism for the disappearance of the contact line proposed in Ref. 40, which is based on an approximate solution of (26), contains a flaw. In Ref. 27 we use the case of the advancing contact angle (6) to show that the method of solution proposed in Ref. 40 cannot correctly predict the nonlinear dependence of the angle on speed. But it is precisely this nonlinear dependence that lies at the heart of the stability analysis of Ref. 40.

The most important extension of the present theory, however, is its application to higher dimensions, in which the contact line no longer remains straight. If a plate withdrawn from a liquid bath is sufficiently wide, the contact line inclines relative to its direction of motion. Two sections of the contact line that have inclined in opposite senses meet at a sharp corner, so that the whole contact line is serrated in an irregular fashion.<sup>38</sup>

A more controlled recent experiment is that of a viscous drop running down an inclined plane.<sup>3</sup> At a critical speed, the initially rounded tail of the drop forms a sharp corner. A recent theory<sup>42</sup> explains the drop profile near the corner of the drop, but not the critical speed at which the corner first occurs, nor its opening angle. To give a complete description of the transition, the microscopic neighborhood of the contact line has to be included, as was done in the present theory for a straight contact line. One important difference between the case of a sliding drop and that of the present paper is that recent experimental evidence suggests that the transition occurs at a finite value of the apparent contact angle.<sup>43</sup> Studies to understand the corner formation of a sliding drop are currently under way.

## ACKNOWLEDGMENTS

I am grateful to Martin Sieber for several important discussions on the matching procedure, to Seth Lichter for improving my physical understanding, and to Lorena Barba for a careful reading of the manuscript. I also acknowledge a very useful conversation with Jacco Snoeijer on transversal perturbations of the contact line.

- <sup>1</sup>D. Quéré, "On the minimal velocity of forced spreading in partial wetting," C. R. Acad. Sci., Ser. II: Mec., Phys., Chim., Sci. Terre Univers **313**, 313 (1991) (in French).
- <sup>2</sup>R. V. Sedev and J. G. Petrov, "The critical condition for transition from steady wetting to film entrainment," Colloids Surf. **53**, 147 (1991).
- <sup>3</sup>T. Podgorski, J. M. Flesselles, and L. Limat, "Corners, cusps, and pearls in running drops," Phys. Rev. Lett. **87**, 036102 (2001).
- <sup>4</sup>P. G. Simpkins and V. J. Kuck, "On air entrainment in coatings," J. Colloid Interface Sci. **263**, 562 (2003).
- <sup>5</sup>D. Quéré, "Fluid coating on a fiber," Annu. Rev. Fluid Mech. **31**, 347 (1999).
- <sup>6</sup>L. D. Landau and E. M. Lifshitz, *Fluid Mechanics* (Pergamon, Oxford, 1984).
- <sup>7</sup>C. Huh and L. E. Scriven, "Hydrodynamic model of steady movement of a solid/liquid/fluid contact line," J. Colloid Interface Sci. **35**, 85 (1971).
- <sup>8</sup>P. A. Thompson and M. O. Robbins, "Simulations of contact-line motion: Slip and the dynamic contact angle," Phys. Rev. Lett. **63**, 766 (1989).
- <sup>9</sup>E. J. Hinch, *Perturbation Methods* (Cambridge University Press, Cambridge, 1991).
- <sup>10</sup>L. M. Hocking, "The spreading of a thin drop by gravity and capillarity," Q. J. Mech. Appl. Math. **36**, 55 (1983).
- <sup>11</sup>P. G. de Gennes, X. Hua, and P. Levinson, "Dynamics of wetting: Local contact angles," J. Fluid Mech. **212**, 55 (1990).
- <sup>12</sup>L. M. Hocking, "The influence of intermolecular forces on thin fluid layers," Phys. Fluids A **5**, 793 (1993).
- <sup>13</sup>J. Eggers, "Hydrodynamic theory of forced dewetting," Phys. Rev. Lett. **93**, 094502 (2004).
- <sup>14</sup>L. M. Hocking, "Meniscus draw-up and draining," Eur. J. Appl. Math. **12**, 195 (2001).
- <sup>15</sup>L. D. Landau and B. V. Levich, "Dragging of a liquid by a moving plate," Acta Physicochim. URSS **17**, 42 (1942).
- <sup>16</sup>B. V. Derjaguin, "On the thickness of a layer of liquid remaining on the walls of vessels after their emptying, and the theory of the application of photoemulsion after coating on the cine film," Acta Physicochim. URSS **20**, 349 (1943).
- <sup>17</sup>P. G. de Gennes, "Wetting: Statics and dynamics," Rev. Mod. Phys. **57**, 827 (1985).
- <sup>18</sup>S. Kistler, "Hydrodynamics of wetting," in *Wettability*, edited by J. C. Berg (Dekker, New York, 1993).
- <sup>19</sup>M. Fermigier and P. Jenffer, "An experimental investigation of the dynamic contact angle in liquid-liquid systems," J. Colloid Interface Sci. **146**, 226 (1991).
- <sup>20</sup>J. A. Marsh, S. Garoff, and E. B. Dussan V., "Dynamic contact angles and hydrodynamics near a moving contact line," Phys. Rev. Lett. **70**, 2778 (1993).
- <sup>21</sup>P. A. Thompson and S. M. Troian, "A general boundary condition for liquid flow at solid surfaces," Nature (London) **389**, 360 (1997).
- <sup>22</sup>J.-H. J. Cho, B. M. Law, and F. Rieutord, "Dipole-dependent slip of Newtonian liquids at smooth solid hydrophobic surfaces," Phys. Rev. Lett. **92**, 166102 (2004).
- <sup>23</sup>S. Lichter, A. Roxin, and S. Mandre, "Mechanisms for liquid slip at solid surfaces," Phys. Rev. Lett. **93**, 086001 (2004).
- <sup>24</sup>O. V. Voinov, "Hydrodynamics of wetting," Fluid Dyn. **11**, 714 (1976) (English translation).
- <sup>25</sup>O. V. Voinov, "Wetting: Inverse dynamic problem and equations for microscopic parameters," J. Colloid Interface Sci. **226**, 5 (2000).
- <sup>26</sup>J. Eggers and H. A. Stone, "Characteristic lengths at moving contact lines for a perfectly wetting fluid: The influence of speed on the dynamic contact angle," J. Fluid Mech. **505**, 309 (2004).
- <sup>27</sup>J. Eggers, "Toward a description of contact line motion at higher capillary numbers," Phys. Fluids **16**, 3491 (2004).
- <sup>28</sup>T. D. Blake and J. M. Haynes, "Kinetics of liquid/liquid displacement," J. Colloid Interface Sci. **30**, 421 (1969).
- <sup>29</sup>A. Prevost, E. Rolley, and C. Guthmann, "Thermally activated motion of

- the contact line of a liquid helium-4 meniscus on a cesium substrate," Phys. Rev. Lett. **83**, 348 (1999).
- <sup>30</sup>F. Brochard-Wyart and P. G. de Gennes, "Dynamics of partial wetting," Adv. Colloid Interface Sci. **9**, 1 (1992).
- <sup>31</sup>R. L. Hoffman, "A study of the advancing interface," J. Colloid Interface Sci. **50**, 228 (1975).
- <sup>32</sup>L. M. Hocking, "Rival contact-angle models and the spreading of drops," J. Fluid Mech. **239**, 671 (1992).
- <sup>33</sup>C. M. Bender and S. A. Orszag, *Advanced Mathematical Methods for Scientists and Engineers* (McGraw-Hill, New York, 1978).
- <sup>34</sup>R. G. Cox, "The dynamics of the spreading of liquids on a solid surface. Part 1. Viscous flow," J. Fluid Mech. **168**, 169 (1986).
- <sup>35</sup>B. R. Duffy and S. K. Wilson, "A third-order differential equation arising in thin-film flows and relevant to Tanner's law," Appl. Math. Lett. **10**, 63 (1997).
- <sup>36</sup>M. Abramowitz and I. A. Stegun, *Handbook of Mathematical Functions* (Dover, New York, 1968).
- <sup>37</sup>B. V. Derjaguin and S. M. Levi, *Film Coating Theory* (Focal, London, 1964).
- <sup>38</sup>T. D. Blake and K. J. Ruschak, "A maximum speed of wetting," Nature (London) **282**, 489 (1979).
- <sup>39</sup>G. Golestanian and E. Raphaël, "Roughening transition in a moving contact line," Phys. Rev. E **67**, 031603 (2003).
- <sup>40</sup>P. G. de Gennes, "Deposition of Langmuir-Blodgett layers," Colloid Polym. Sci. **264**, 463 (1986).
- <sup>41</sup>Y. Pomeau, "Recent progress in the moving contact line problem: A review," C. R. Mécanique **330**, 207 (2002).
- <sup>42</sup>L. Limat and H. A. Stone, "Three-dimensional lubrication model of a contact line corner singularity," Europhys. Lett. **65**, 365 (2004).
- <sup>43</sup>N. Le Grand, A. Daerr, and L. Limat, "Shape and motion of drops sliding down an inclined plane," J. Fluid Mech. (to be published).